Progress In Electromagnetics Research M, Vol. 32, 157–167, 2013

AN EFFICIENT SCHEME FOR ANALYSIS OF ELECTROMAGNETIC SCATTERING FROM TARGET AND ENVIRONMENT COMPOSITE MODEL

Min Wang[1, *], Jialin Chen[2], and Yanjie Cao[3]

[1]Department of Ordnance Science and Technology, Naval Aeronautical and Astronautical University, Yantai 264001, China

[2]Department of Electronic and Information Engineering, Naval Aeronautical and Astronautical University, Yantai 264001, China

[3]Department of Command, Naval Aeronautical and Astronautical University, Yantai 264001, China

Abstract—We present an efficient scheme for the analysis of electromagnetic scattering from target and environment composite model. In this scheme, the whole computed domain is divided into a target part and an environment part, and each part is formulated by different integral equations. The two parts are solved one by one until the relative residual error is less than a given value. Compared with conventional solution with pure electric field integral equation (EFIE), the proposed scheme has a better convergence and lower memory requirement. Additionally, the multilevel fast multipole algorithm (MLFMA) is utilized to accelerate the computations of matrix vector product. Simulated radar-cross-section (RCS) results of several examples demonstrate its validity and efficiency.

1. INTRODUCTION

A target with high velocity may be intercepted difficultly. Additionally, if the target has a low flight altitude, it will be difficult to be found from the environment. In order to implement target detection and tracking, the analysis of electromagnetic (EM) scattering from target and environment composite model becomes important. Actually, the method of moments (MoM) solutions of surface integral equations (SIEs) are widely used for numerical analysis of EM radiation and

Received 19 June 2013, Accepted 10 August 2013, Scheduled 13 August 2013

* Corresponding author: Min Wang (min6622949@sina.com).

scattering problems [1–9]. For these EM scattering problems of composite model, the formulation is achieved by electric field integral equation (EFIE) with no choice because of the presence of open surfaces of environment. It is well known that the EFIE can be used with MoM to treat problems of scattering by arbitrarily shaped objects [10]. However, the EFIE is prone to internal resonance problems and leads to ill-conditioned matrix equations that decrease convergence rate of iterative solvers. The hybrid CFIE-EFIE [11, 12] can be used to accelerate the convergence rate of iterations, but they are usually problem-dependent. The hybrid methods combining MoM with asymptotic techniques [13, 14] are efficient, but they have the shortcoming of low accuracy.

In this paper, an efficient scheme is proposed to improve the solutions of these scattering problems. In this scheme, the whole computed domain is divided into a closed part and an open part, which correspond to the target and environment parts. The closed part is formulated by combined field integral equation (CFIE) [15], and the open part is formulated by EFIE. According to the MoM procedure [10], there will be two sub-matrix equations. The two sub-matrix equations are solved one by one until the relative residual error is less than a given value. Compared with conventional solution with pure EFIE, the proposed scheme has better convergence and lower memory requirement. Additionally, the multilevel fast multipole algorithm (MLFMA) [15–23] is utilized to accelerate the computations of matrix vector product. Numerical examples have demonstrated the validity and efficiency of the proposed scheme.

2. FORMULATIONS

For composite model with target and environment, the conventional EFIE solutions become inefficient due to the presence of open surfaces. We improve solutions of these problems by taking a hint from the improvement by the CFIE in the solution of scattering problems involving only closed surfaces. The basic idea of the proposed scheme is to divide the computed domain into closed and open parts, then use different integral equations in different parts flexibly and solve two sub-matrix equations. The proposed scheme is time-saving and memory-saving compared with the conventional solutions.

In this paper, we consider the solution of the scattering problems involving both closed and open conducting surfaces, which are illuminated by plane wave. The EFIE and magnetic field integral equation (MFIE) with respect to the induced current on the surface S

can be written as

$$\hat{\mathbf{t}}\cdot jk_0\eta_0\left[\int_S \mathbf{J}(\mathbf{r}')g(\mathbf{r},\mathbf{r}')ds' + \frac{\nabla}{k_0^2}\int_S \nabla\cdot\mathbf{J}(\mathbf{r}')g(\mathbf{r},\mathbf{r}')ds'\right] = \hat{\mathbf{t}}\cdot\mathbf{E}^i(\mathbf{r}), \quad (1)$$

and

$$\hat{\mathbf{t}}\cdot\left[\frac{1}{2}\mathbf{J}(\mathbf{r}') - \hat{\mathbf{n}}\times\nabla\times\int_S ds'g(\mathbf{r},\mathbf{r}')\mathbf{J}(\mathbf{r}')\right] = \hat{\mathbf{t}}\cdot\hat{\mathbf{n}}\times\mathbf{H}^i(\mathbf{r}) \quad (2)$$

where $\hat{\mathbf{t}}$ is any unit tangent vector on surface; $\hat{\mathbf{n}}$ is the unit outward normal vector of the conductor surface; k_0 and η_0 are the wavenumber and wave impedance of free space; $\mathbf{J}$ is the surface current; $\mathbf{r}'$ and $\mathbf{r}$ denote the locations of source and observation point, respectively; $g(\mathbf{r},\mathbf{r}') = e^{-jk|r-r'|}/4\pi\,|\mathbf{r}-\mathbf{r}'|$ is the Green's function of free space; $\mathbf{E}^i$ and $\mathbf{H}^i$ denote the incident electric field and magnetic field respectively.

To accelerate the convergence and reduce the memory requirement, an efficient scheme is proposed. Its basic principle may be described using Figure 1, where the whole computed domain is divided into target domain and environment domain. For simplicity, the whole computed domain is defined as Ω, the target domain i defined as Ω_T, the environment domain defined as Ω_E, and $\Omega = \Omega_T + \Omega_E$.

For the environment domain Ω_E, we define two linear operators $T_{EE}(\mathbf{r},\,\mathbf{J})$ and $F_{EE}(\mathbf{r},\,\mathbf{J})$ with respect to EFIE as

$$T_{EE}(\mathbf{r},\mathbf{J}) = \hat{\mathbf{t}}\cdot jk_0\eta_0\left[\int_{\Omega_E}\mathbf{J}(\mathbf{r}')g(\mathbf{r},\mathbf{r}')ds' + \frac{\nabla}{k_0^2}\int_{\Omega_E}\nabla\cdot\mathbf{J}(\mathbf{r}')g(\mathbf{r},\mathbf{r}')ds'\right], \quad \mathbf{r}'\in\Omega_E,\ \ \mathbf{r}\in\Omega_E, \quad (3)$$

$$F_{EE}(\mathbf{r},\mathbf{J}) = \hat{\mathbf{t}}\cdot jk_0\eta_0\left[\int_{\Omega_T}\mathbf{J}(\mathbf{r}')g(\mathbf{r},\mathbf{r}')ds' + \frac{\nabla}{k_0^2}\int_{\Omega_T}\nabla\cdot\mathbf{J}(\mathbf{r}')g(\mathbf{r},\mathbf{r}')ds'\right], \quad \mathbf{r}'\in\Omega_T,\ \ \mathbf{r}\in\Omega_E, \quad (4)$$

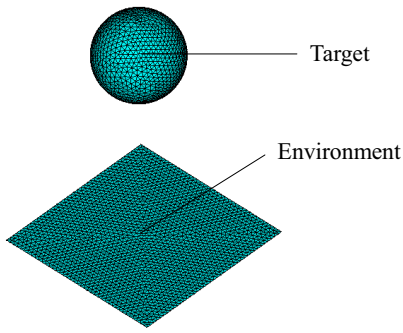

Figure 1. The illustration of target and environment composite model.

then the iterative scheme of Ω_E can be expressed as

$$T_{EE}\left(\mathbf{r}, \mathbf{J}^{(k)}\right) = -F_{EE}\left(\mathbf{r}, \mathbf{J}^{(k-1)}\right) + \hat{\mathbf{t}} \cdot \mathbf{E}^i(\mathbf{r}), \quad \mathbf{r} \in O_E. \tag{5}$$

According to the MoM procedure, the whole conductor surface S is first discretized into triangles, and then the induced current $\mathbf{J}$ on the surface S is expanded by using RWG basis functions. By applying Galerkin's testing, Equation (5) is converted into the following matrix equation

$$Z_{EE} I_E^{(k)} = V_E - Z_{ET} I_T^{(k-1)} \tag{6}$$

where the V_E is the vector of the incident field in Ω_E, $I_E^{(k)}$ the vector of the current coefficients in Ω_E to be solved during the kth iteration, and $I_T^{(k-1)}$ the vector of the current coefficients in Ω_T after being solved at the $(k-1)$th iteration. Z_{EE} and Z_{ET} are the self-impedance matrix in Ω_E and the mutual-impedance matrix between Ω_E and Ω_T, respectively.

Similarly, for target domain Ω_T, we define four linear operators, where $T_{TE}(\mathbf{r}, \mathbf{J})$ and $F_{TE}(\mathbf{r}, \mathbf{J})$ are relevant to EFIE, while $T_{TM}(\mathbf{r}, \mathbf{J})$ and $F_{TM}(\mathbf{r}, \mathbf{J})$ are relevant to MFIE. These operators are expressed as

$$T_{TE}(\mathbf{r}, \mathbf{J}) = \hat{\mathbf{t}} \cdot jk_0\eta_0 \left[\int_{\Omega_T} \mathbf{J}(\mathbf{r}') g(\mathbf{r}, \mathbf{r}') ds' + \frac{\nabla}{k_0^2} \int_{\Omega_T} \nabla \cdot \mathbf{J}(\mathbf{r}') g(\mathbf{r}, \mathbf{r}') ds' \right], \quad \mathbf{r}' \in \Omega_T, \ \mathbf{r} \in \Omega_T, \tag{7}$$

$$F_{TE}(\mathbf{r}, \mathbf{J}) = \hat{\mathbf{t}} \cdot jk_0\eta_0 \left[\int_{\Omega_E} \mathbf{J}(\mathbf{r}') g(\mathbf{r}, \mathbf{r}') ds' + \frac{\nabla}{k_0^2} \int_{\Omega_E} \nabla \cdot \mathbf{J}(\mathbf{r}') g(\mathbf{r}, \mathbf{r}') ds' \right], \quad \mathbf{r}' \in \Omega_E, \ \mathbf{r} \in \Omega_T, \tag{8}$$

$$T_{TM}(\mathbf{r}, \mathbf{J}) = \hat{\mathbf{t}} \cdot \left[\frac{1}{2} \mathbf{J}(\mathbf{r}) - \hat{\mathbf{n}} \times \nabla \times \int_{\Omega_T} ds' g(\mathbf{r}, \mathbf{r}') \mathbf{J}(\mathbf{r}') \right], \quad \mathbf{r}' \in \Omega_T, \ \mathbf{r} \in \Omega_T, \tag{9}$$

$$F_{TM}(\mathbf{r}, \mathbf{J}) = \hat{\mathbf{t}} \cdot \left[\hat{\mathbf{n}} \times \nabla \times \int_{\Omega_E} ds' g(\mathbf{r}, \mathbf{r}') \mathbf{J}(\mathbf{r}') \right], \ \mathbf{r}' \in \Omega_E, \ \mathbf{r} \in \Omega_T. \tag{10}$$

The iterative scheme of Ω_T can be expressed as

$$\alpha T_{TE}\left(\mathbf{r}, \mathbf{J}^{(k)}\right) + (1-\alpha)\eta_0 T_{TM}\left(\mathbf{r}, \mathbf{J}^{(k)}\right) = \alpha \left[-F_{TE}\left(\mathbf{r}, \mathbf{J}^{(k-1)}\right) + \hat{\mathbf{t}} \cdot \mathbf{E}^i(\mathbf{r}) \right]$$
$$+ (1-\alpha)\eta_0 \left[F_{TM}\left(\mathbf{r}, \mathbf{J}^{(k-1)}\right) + \hat{\mathbf{t}} \cdot \hat{\mathbf{n}} \times \mathbf{H}^i(\mathbf{r}) \right], \quad \mathbf{r} \in \Omega_T. \tag{11}$$

As Equation (5), Equation (11) can be converted into the following matrix equation

$$Z_{TT} I_T^{(k)} = V_T - Z_{TE} I_E^{(k)}, \tag{12}$$

where V_T is a vector containing the information of the incident electric field and magnetic field in the Ω_T, $I_T^{(k)}$ the vector of the current coefficients in Ω_T to be solved during the kth iteration, $I_E^{(k)}$ the vector of the current coefficients in Ω_E after being solved at the kth iteration, and both the self-impedance matrix Z_{TT} and the mutual-impedance matrix Z_{TE} contain the information of electric field and magnetic field.

The sub-matrix Equations (6) and (12) can be solved one by one until the relative residual error is less than a given value. In order to increase efficiency of the proposed scheme, the MLFMA is used to speed up the matrix vector product in Equations (6) and (12). The basic idea of the MLFMA is to convert the interaction of element-to-element to the interaction of cube-to-cube. We first select the smallest cube in three dimensions containing the entire domain composed of RWG basis function elements and partition it into eight subcubes. Each subcube is then recursively subdivided into eight smaller cubes until the edge length of the cube is about 0.25 wavelength, which is controllable. As a result, all the basis function elements are assigned in the cubes. The illustration of partition is shown in Figure 2.

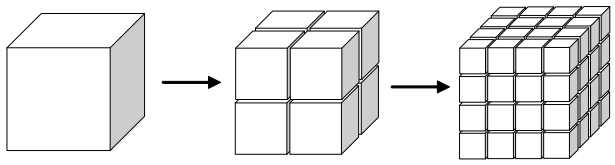

Figure 2. The illustration of partition in MLFMA.

We expound the application of the MLFMA in Equation (6), and Equation (12) is similar. In Equation (6), the matrix vector product $Z_{EE}I_E^{(k)}$ for interactions inside Ω_E is accelerated by the conventional MLFMA, in which the direct interaction between two far-field elements is separated into three steps containing aggregation, translation and disaggregation. $Z_{ET}I_T^{(k-1)}$ represents the interaction between Ω_T and Ω_E, so the excitation source in the computed domain Ω_E includes both the information of plane wave and the coupling from Ω_T. It is different from the conventional MLFMA to accelerate the $Z_{ET}I_T^{(k-1)}$, where the aggregation arises in Ω_T, the translation from Ω_T to Ω_E, and the disaggregation in the Ω_E.

3. NUMERICAL EXAMPLES

In this section, several numerical examples are presented to illustrate the validity and efficiency of the proposed scheme. In these examples, the relative residual errors of iteration solution of Equations (6) and (12) are set as 0.0001. It should be noted that the MLFMA is used in each simulation of these examples to accelerate the matrix vector product computations. All the computations are performed on a PC with Intel Dual-core 2.5 GHz CPU and 4 GB RAM in double precision.

The relative residual error at the kth iteration is used for monitoring the convergence of the proposed method, which is defined as

$$\varepsilon(V,k) = \frac{\left|\left|V - ZI^{(k)}\right|\right|_2}{||V||_2} \tag{13}$$

where $||\cdot||_2$ denotes the 2-norm of the complex vector. The iteration stops when $\varepsilon(V,k)$ is less than 0.0001.

As the first example, a composite model with coexisting closed sphere and open square plate is considered to check the accuracy of the proposed method. As shown in Figure 1, the radius of the sphere is λ, the edge length of the plate 4λ, and the distance between the sphere and the plate 5λ. The incident angles are Theta = 150° and Phi = 180°. Figure 3 shows that the bistatic RCS results at Phi = 0° and Phi = 90° computed by the proposed method agree well with the results computed by using only the EFIE formulation.

The second example is a composite model composed of an armature of electromagnetic launcher (EML) and a Gaussian rough

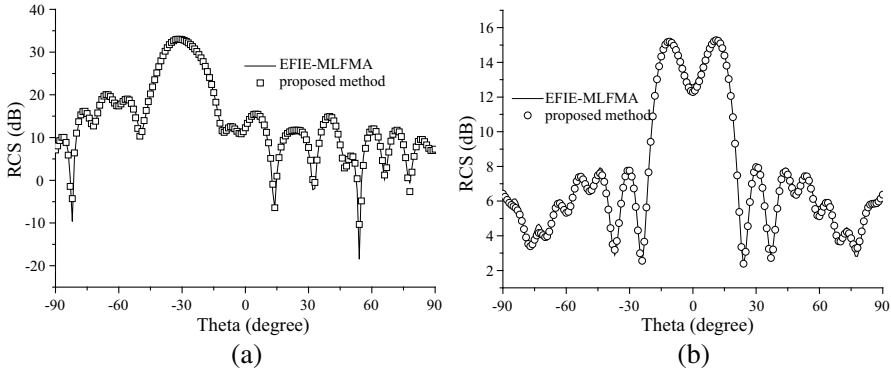

Figure 3. Simulated bistatic RCS results of the first example. (a) phi = 0°, (b) phi = 90°.

surface environment with the following Gaussian spectrum.

$$W(k_x, k_y) = \frac{l_x l_y h^2}{4\pi} e^{-\frac{l_x^2 k_x^2 + l_y^2 k_y^2}{4}} \tag{14}$$

Here, l_x and l_y are the correlation lengths in x-direction and y-direction, respectively, and h is the root-mean-square height of the rough surface. The specific size of armature is marked in Figure 4. The size of the Gaussian rough surface is $4\lambda * 4\lambda$. The root-mean-square height and correlation length of the rough surface are $h = 0.05\lambda$ and $l_x = l_y = 1.2\lambda$, respectively. The distance between the armature and the rough surface is 5λ. The incident angles are Theta $= 150°$ and Phi $= 180°$. Figure 5 shows the RCS results at Phi $= 0°$ and Phi $= 90°$ computed by the proposed method and the pure EFIE. It can be seen that the results are in good agreement.

The third example is a composite model with lying cylinder and square plate, which denote the target and environment parts. The

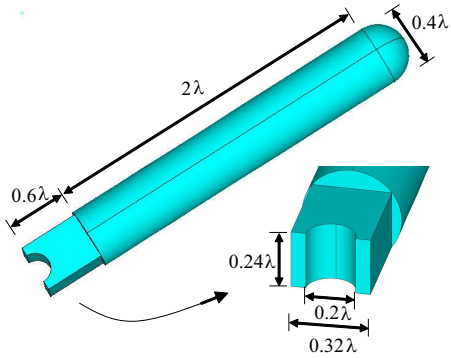

Figure 4. The specific size of armature.

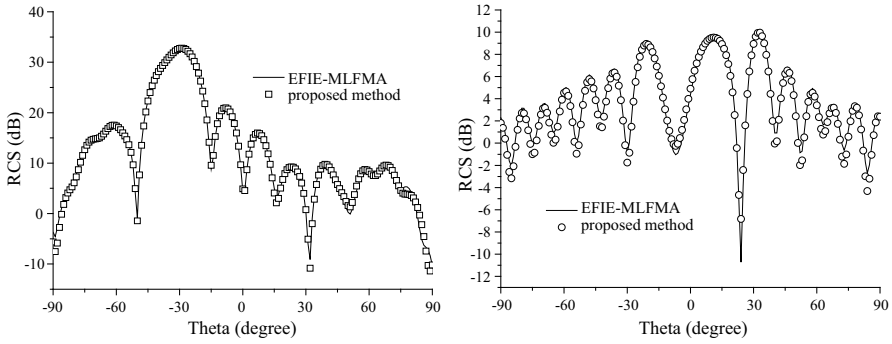

Figure 5. Simulated bistatic RCS results of the second example. (a) phi $= 0°$, (b) phi $= 90°$.

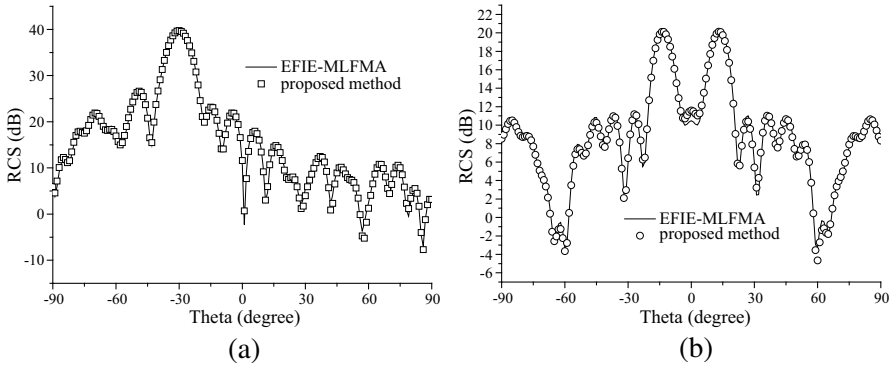

Figure 6. Simulated bistatic RCS results of the third example. (a) phi = 0°, (b) phi = 90°.

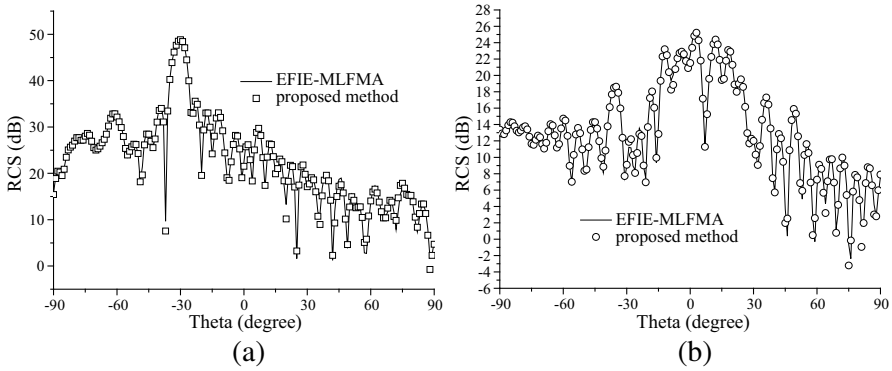

Figure 7. Simulated bistatic RCS results of the fourth example. (a) phi = 0°, (b) phi = 90°.

sizes of the cylinder and square plate are $3\lambda * 2\lambda * 2\lambda$ and $6\lambda * 6\lambda$. The corresponding numbers of unknowns are 8439 and 12195, and their distance is 6λ. The incident angles are Theta = 150° and Phi = 180°. Figure 6 shows the RCS results at Phi = 0° and Phi = 90°.

The fourth example is a composite model with a larger lying cylinder and a larger Gaussian rough surface. The sizes of the cylinder and the rough surface are $6\lambda * 4\lambda * 4\lambda$ and $12\lambda * 12\lambda$. The corresponding numbers of unknowns are 34383 and 42960, and their distance is 10λ. The root-mean-square height and correlation lengths of the rough surface are $h = 0.05\lambda$ and $l_x = l_y = 1.0\lambda$, respectively. The incident angles are Theta = 150° and Phi = 180°. Figure 7 shows the RCS results at Phi = 0° and Phi = 90°.

The computational costs of the four examples are shown in

Table 1. Computational costs of the four examples.

	Methods	Number of unknowns		Memory requirement (MB)	Total CPU time
Example 1	EFIE-MLFMA	9217		73.7 MB	237 s
	Proposed method	Target	Environment	32.3 MB	71 s
		3849	5368		
Example 2	EFIE-MLFMA	5881		36.7 MB	309 s
	Proposed method	Target	Environment	22.3 MB	54 s
		1161	4720		
Example 3	EFIE-MLFMA	20634		81.6 MB	1633 s
	Proposed method	Target	Environment	38.9 MB	234 s
		8439	12195		
Example 4	EFIE-MLFMA	77343		632.6 MB	$>$ 6 days
	Proposed method	Target	Environment	328.8 MB	1259 s
		34383	42960		

Table 1. By applying the proposed scheme, the memory requirements and total CPU time are dramatically reduced compared to the pure EFIE. When the problems become larger, the effects are more obvious.

4. CONCLUSION

In this paper, a novel scheme is presented for the solution of the composite problems with target and environment. Numerical examples have demonstrated that the proposed scheme has improved the solution efficiency and reduced the memory requirements significantly compared to using only the EFIE formulation on the whole geometry. As the problem size gets larger, the improved convergence provided by the proposed scheme becomes critically important. The idea of using different integral equations to treat the different parts can be extended to the future research.

REFERENCES

1. Michalski, K. A. and D. L. Zheng, "Electromagnetic scattering and radiation by surfaces of arbitrary shape in layered media, Part I: Theory," *IEEE Trans. on Antennas and Propag.*, Vol. 38, No. 3, 335–344, Mar. 1990.
2. Michalski, K. A. and D. L. Zheng, "Electromagnetic scattering and radiation by surfaces of arbitrary shape in layered media, Part II: Implementation and results for contiguous half-spaces," *IEEE Trans. on Antennas and Propag.*, Vol. 38, No. 3, 345–352, Mar. 1990.

3. Engheta, N., W. D. Murphy, V. Rokhlin, and M. S. Vassiliou, "The fast multipole method (FMM) for electromagnetic scattering problems," *IEEE Trans. on Antennas and Propag.*, Vol. 40, No. 6, 634–641, Jun. 1992.
4. Coifman, R., V. Rokhlin, and S. M. Wandzura, "The fast multipole method (FMM) for the wave equation: A pedestrian prescription," *IEEE Trans. on Antennas and Propag.*, Vol. 35, No. 3, 7–12, Jun. 1993.
5. Chen, J., S. Li, and M. Wang, "Targets identification method based on electromagnetic scattering analysis," *2011 IEEE CIE International Conference on Radar*, Vol. 2, 1647–1651, Oct. 2011.
6. Chen, J., S. Li, and Y. Song, "Analysis of electromagnetic scattering problems by means of a VSIE-ODDM-MLFMA method," *ACES Journal*, Vol. 27, No. 8, 660–667, Aug. 2012.
7. Chen, J., M. Wang, S. Li, M. Zhu, J. Yu, and X. Li, "An IE-ODDM scheme combined with efficient direct solver for 3D scattering problems," *Micro. Opt. Tech. Lett.*, Vol. 55, No. 9, 2027–2033, Sep. 2013.
8. Chang, X. and L. Tsang, "A new efficient method for modeling dense via arrays with 1D method of moment and group T matrix," *2012 Electrical Performance of Electronic Packaging International Symposium*, 163–166, Tempe, AZ, USA, Oct. 2012.
9. Tsang, L. and X. Chang, "Modeling of vias sharing the same antipad in planar waveguide with boundary integral equation and group T matrix method," *IEEE Transactions on Components, Packaging and Manufacturing Technology*, Vol. 3, 315–327, Feb. 2013.
10. Rao, S. M., D. R. Wilton, and A. W. Glisson, "Electromagnetic scattering by surface of arbitrary shape," *IEEE Trans. on Antennas and Propag.*, Vol. 30, No. 3, 409–418, May 1982.
11. Ergül, Ö. and L. Gürel, "Hybrid CFIE-EFIE solution of composite geometries with coexisting open and closed surfaces," *IEEE Antennas Propag. Symp.*, Vol. 4B, 289–292, Jul. 2005.
12. Gürel, L. and Ö. Ergül, "Extending the applicability of the combined-field integral equation to geometries containing open surfaces," *IEEE Antennas and Wirel. Propag. Lett.*, Vol. 5, 515–516, 2006.
13. Jakobus, U. and F. M. Landstorfer, "Improved PO-MM hybrid formulation for scattering from three-dimensional perfectly conducting bodies of arbitrary shape," *IEEE Trans. on Antennas and Propag.*, Vol. 43, No. 2, 162–169, Feb. 1995.

14. Chen, H. T., G. Q. Zhu, J. X. Luo, and F. Yuan, "A modified MoM-PO method for analyzing wire antennas near to coated PEC plates," *IEEE Trans. on Antennas and Propag.*, Vol. 56, No. 6, 1818–1822, Jun. 2008.
15. Song, J. M. and W. C. Chew, "Multilevel fast-multipole algorithm for solving combined field integral equation of electromagnetic scattering," *Micro. Opt. Tech. Lett.*, Vol. 10, No. 1, 14–19, Sep. 1995.
16. Lu, C. C. and W. C. Chew, "A multilevel algorithm for solving boundary integral equations of wave scattering," *Micro. Opt. Tech. Lett.*, Vol. 7, No. 10, 466–470, Jul. 1994.
17. Song, J. M., C. C. Lu, and W. C. Chew, "Multilevel fast multipole algorithm for electromagnetic scattering by large complex objects," *IEEE Trans. on Antennas and Propag.*, Vol. 45, No. 10, 1488–1493, Oct. 1997.
18. Shao, H., J. Hu, Z.-P. Nie, G. Han, and S. He, "Hybrid tangential equivalence principle algorithm with MLFMA for analysis of array structures," *Progress In Electromagnetics Research*, Vol. 113, 127–141, 2011.
19. Ping, X. W., T.-J. Cui, and W. B. Lu, "The combination of BCGSTAB with multifrontal algorithm to solve FEBI-MLFMA linear systems arising from inhomogeneous electromagnetic scattering problems," *Progress In Electromagnetics Research*, Vol. 93, 91–105, 2009.
20. Peng, Z., X.-Q. Sheng, and F. Yin, "An efficient twofold iterative algorithm of FE-BI-MLFMA using multilevel inverse-based ILU preconditioning," *Progress In Electromagnetics Research*, Vol. 93, 369–384, 2009.
21. Wallén, H. and J. Sarvas, "Translation procedures for broadband MLFMA," *Progress In Electromagnetics Research*, Vol. 55, 47–78, 2005.
22. Islam, S., J. Stiens, G. Poesen, R. Vounckx, J. Peeters, I. Bogaert, D. de Zutter, and W. de Raedt, "Simulation and experimental verification of w-band finite frequency selective surfaces on infinite background with 3D full wave solver NSPWMLFMA," *Progress In Electromagnetics Research*, Vol. 101, 189–202, 2010.
23. Taboada, J. M., M. G. Araújo, J. M. Bértolo, L. Landesa, F. Obelleiro, and J. L. Rodriguez, "MLFMA-FFT parallel algorithm for the solution of large-scale problems in electromagnetics (invited paper)," *Progress In Electromagnetics Research*, Vol. 105, 15–30, 2010.